

shift considerably less than  $\pi/2$ , and the residual cross section at the minimum may not be in disagreement with that expected from the hard-sphere approximation of potential scattering.

#### IV. SUMMARY

A summary of the information concerning the narrow energy levels discussed in Sec. III is given in Table I. For the sake of completeness, the resonances described in references 5 and 7 are included in this table. The first column lists the compound nuclei studied, together with the binding energy of the neutron,  $E_b$ . In the next four columns the resonance energies,  $E_r$ , the excitation energies  $E_{ex}$ , the observed widths  $\Gamma$ , corrected for experimental resolution, and the total angular momenta  $J$  are given. In the assignment of values of  $J$  it has been assumed that the resonances are entirely due to elastic scattering. Available experimental data indicate that for the nuclei listed in Table I, processes other than elastic scattering are probably negligible in the energy range under investigation. The unresolved resonances

are also tabulated together with the lower bounds of their total angular momenta and the upper limits of their widths. For these maxima, no correction for experimental resolution has been applied.

The reduced widths,<sup>19</sup>  $\gamma^2$ , of the levels listed in Table I have been computed for values of the orbital angular momentum,  $l$ , which have been shown to be reasonable in the previous section. Since the calculation of reduced widths is sensitive to the interaction radius,  $a$ , the computation has been performed for two values of  $a$ . The observed widths have been corrected for the variation of the level shift with energy.<sup>17</sup> Also included in Table I is the ratio of the reduced widths to the sum-rule limit,<sup>19</sup>  $3\hbar^2/2Ma$ , where  $M$  is the reduced mass of the system. Values of  $l$  which result in reduced widths exceeding the sum rule limit for the interaction radii used are shown in parentheses and can probably be excluded. In addition, those values of  $l$  yielding reduced widths which are large fractions of  $3\hbar^2/2Ma$  are not likely to be applicable.

<sup>19</sup> E. P. Wigner, Am. J. Phys. 17, 99 (1949).

## Energy Distribution of Fission Fragments of $U^{235}$ Produced by 2.5-Mev and 14-Mev Neutrons\*

STEPHEN S. FRIEDLAND†

*University of California, Los Alamos Scientific Laboratory, Los Alamos, New Mexico*

(Received February 19, 1951)

The kinetic energy released in the fission of  $U^{235}$  by 2.5-Mev and 14-Mev neutrons has been measured. The results show the familiar two-peak curve when intensity of a fragment with a given energy is plotted against energy. However, the dip between the peaks apparently disappears with increasing energy of the neutrons and the distribution approaches a single symmetrical peak.

#### INTRODUCTION

SEVERAL investigators have studied the kinetic energy released by the fission of  $U^{235}$  when induced by thermal neutrons.<sup>1-4</sup> Their results showed the now familiar double peak curve when the intensity of fission fragments with a given energy is plotted against the kinetic energy of the fragments. Recently Jungerman and Wright<sup>5</sup> studied the energy released in the fission process when neutrons at 90 Mev and 45 Mev are used. Their 45-Mev data showed a large decrease in the size of the dip between the two peaks, whereas their 90-Mev data showed no dip whatsoever but a single peak curve. This paper reports on the results of measurements taken when fission is induced in  $U^{235}$  by 2.5-Mev and 14-Mev neutrons.

\* Work done under the auspices of the AEC.

† Now at the University of Connecticut, Department of Physics, Storrs, Connecticut.

<sup>1</sup> W. Jentschke, Z. Physik, 120, 165 (1943).

<sup>2</sup> A. Flammersfeld, Z. Physik 120, 450 (1943).

<sup>3</sup> M. Deutsch, MDDC-945 (unpublished).

<sup>4</sup> J. L. Fowler and L. Rosen, Phys. Rev. 72, 926 (1947).

<sup>5</sup> J. Jungerman and S. C. Wright, Phys. Rev. 76, 1112 (1949).

#### EXPERIMENTAL METHOD

The method used in this experiment was essentially the same as that used by other investigators, that is, the ionization produced in an ionization chamber by the fission fragments was compared to the ionization produced by alpha-particles of a known energy. An

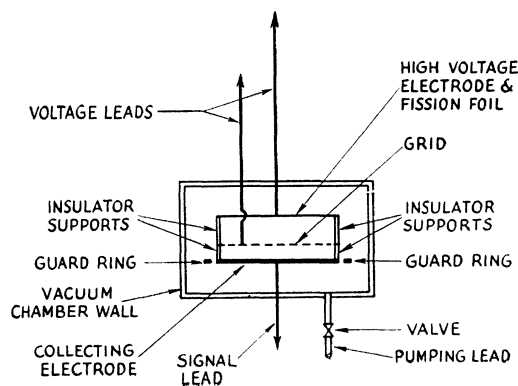


FIG. 1. Schematic diagram of ionization chamber

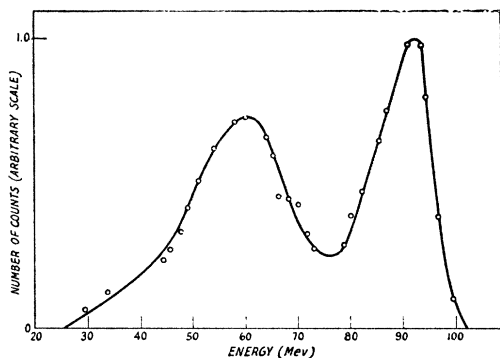


FIG. 2. Energy spectrum of  $U^{235}$  fission fragments induced by thermal neutrons.

ionization chamber designed by Fowler and Rosen, and similar to the one described in their paper,<sup>4</sup> was used. The details of the construction may be found in their paper. The chamber, Fig. 1, was of the electron-collection type. The screen, which shields the collecting electrode from the positive ions, was one cm from the

TABLE I. Data on high and low energy fission products.

	Position of high energy peak	Position of low energy peak	Ratio of minimum to high energy peak (per cent)	Ratio of high energy peak to low energy peak	Foil thickness (mg/cm <sup>2</sup> )
$U^{235}$ thermal neutrons					
Fowler and Rosen	93	61.8	21	1.50	0.105
Friedland	93	60.1	23	1.54	0.140
$U^{235}$ 2.5-Mev neutrons	91	59	36	1.5	0.140
$U^{235}$ 14-Mev neutrons	91	59	57	1.5	0.140

collecting electrode and 2.2 cm from the high voltage electrode. The high voltage electrode, upon which was deposited the fissionable material, was maintained at 4000 volts while the grid was maintained at 1850 volts. The high field region between the grid and the collecting electrode was established to insure the "funnel effect"<sup>13</sup> for the electrons through the grid wires. The chamber

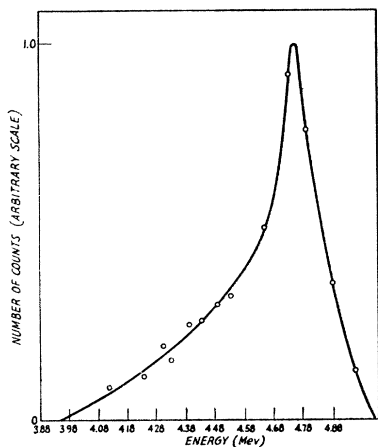


FIG. 3. Energy distribution of  $U^{234}$  alpha-particles.

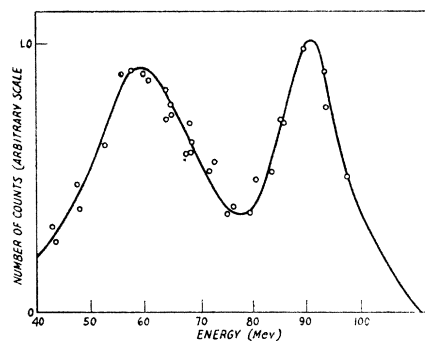


FIG. 4. Energy spectrum of  $U^{235}$  fission fragments induced by 2.5-Mev neutrons.

was filled to a total pressure of 162 cm of mercury of which 95 percent was argon and 5 percent was  $CO_2$ . This pressure was more than sufficient to stop the longest range fission fragments, as well as the calibrating alpha particles before they reached the grid. The  $CO_2$  was present to hasten the collection time of the ions. The gas was continuously purified by passing it over calcium metal which was heated to 180°C.

The pulse obtained from the chamber was amplified with a Model 100 preamplifier before passing on to the amplifier.<sup>6</sup>

A clipping circuit, consisting of a 3- $\mu$ sec delay line was used to place on the grid of the amplifier the original signal which had been inverted by reflection. The amplified signal was fed into a 10-channel pulse amplitude analyzer,<sup>6</sup> which had been adjusted to have each channel accept pulses over equal ranges. For the amplification used the channel widths were set either at 0.8 Mev or 2.0 Mev. By shifting the bias on the analyzer, it was possible to cover the entire range of the fission pulses, taking nine points at a time. Because of the tendency of the 10-channel analyzer to drift, it was calibrated before and after each run.

The neutron source used was the Los Alamos Cockroft-Walton set. For the 14-Mev neutrons the  $H^3(H^2, n)He^4$  reaction was used, while for the 2.5-Mev neutrons the  $H^2(H^2, n)He^3$  reaction was used.

The fission foil was made by John Povelites and

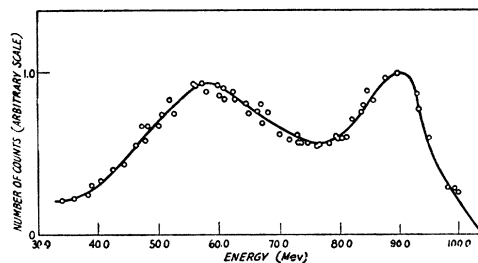


FIG. 5. Energy spectrum of  $U^{235}$  fission fragments induced by 14-Mev neutrons.

<sup>6</sup> W. C. Elmore and M. Sands, *Electronics: Experimental Techniques* (McGraw-Hill Book Company, Inc., New York, 1949).

had a foil thickness of  $0.14 \text{ mg/cm}^2$  and a total weight of  $5.42 \text{ mg}$ .

To check the apparatus and the techniques required for the experiment, a thermal source of neutrons was obtained by placing a Po-Be source in a graphite pile and the distribution of the energy of the fission fragments was obtained. The results are shown in Fig. 2 and are compared to the results of Fowler and Rosen<sup>4</sup> in Table I.

The distribution of the energy of ionization produced by the alpha-particles of  $U^{234}$  is shown in Fig. 3. The width at half maximum serves as a measure of the resolution of the ionization chamber and is approximately  $0.2 \text{ Mev}$ .

## RESULTS

Figures 4 and 5 show the energy distribution of the fission fragments for  $U^{235}$  when induced by neutrons of  $2.5 \text{ Mev}$  and  $14 \text{ Mev}$ , respectively. Table I compares these with results obtained with thermal neutrons.

The data obtained is in agreement with those of Jungerman and Wright. The dip between the peaks apparently disappears with increasing energy and the distribution approaches a single symmetrical peak.

Acknowledgments are due Mr. R. W. Davis for operating the Cockroft-Walton set and Drs. J. H. Coon, J. L. Fowler, E. R. Graves and L. Rosen for many discussions.

## Absorption Length and Collision Length of Hard-Shower-Producing Radiation

DAVID POMEROY\*

*University of New Mexico, Albuquerque, New Mexico*

(Received February 23, 1951)

By combining techniques of coincidence counter circuits and nuclear photographic emulsions, values are obtained for the absorption length in air of  $104 \pm 6$  (p.e.)  $\text{g/cm}^2$ , and for the collision length in paraffin of  $61 \pm 6$  (p.e.)  $\text{g/cm}^2$  for hard-shower-producing radiation. The method also provides evidence of a cascade mechanism by which the hard showers are produced.

TWO experiments have been conducted in order to obtain the values of the absorption length in air, and of the collision length in paraffin, for the hard-shower-producing component of cosmic radiation. The results provide evidence on how the hard showers are produced. Both experiments were performed at two elevations, namely, at 5200 feet (University of New Mexico) and at 10,700 feet (Sandia Crest, New Mexico), referred to as "roof" and "crest" in the sequence, respectively. The first experiment made use of photographic emulsions, while the second experiment utilized the techniques of counter tube circuits.

### FIRST EXPERIMENT

Two dozen Ilford G5 plates ( $200\mu$  emulsion thickness) were exposed to cosmic radiation at each of the two elevations. In each case one dozen plates were placed vertically under a hemisphere of paraffin of radius 38 cm, with the other dozen near by without shielding. After 10 to 14 days exposure, the plates were processed by the method reported by Dilworth, Occhialini, and Payne.<sup>1</sup> The plates were then subjected to microscopic examination for the detection of hard showers.

Since the showers always formed part of stars, counts were also made of stars with 5 or more prongs whether they were accompanied by hard showers or not. Radioactive contamination stars were eliminated by the

criterion that at least one of the prongs of the 5 prong stars had to exceed  $55\mu$  in length.

Preliminary examination was made under low magnification ( $10\times$  objective). In order to check on the accuracy of this procedure, tests were made on the number of stars found at different scanning rates, using an old Ilford C2 plate which had been in a drawer for several months, so that the star density was relatively high. The results are shown in Table I.

The final results are based on a 9 hour scanning time per plate under low power. Every star accepted was later examined under oil immersion ( $95\times$  objective) for hard showers.

A listing of the number of stars and hard showers found at the two different altitudes with and without absorber is given in Tables II and III. From the data given in those tables we calculate the standard deviations listed in Table IV.

From Tables II and IV we obtain the altitude dependence and calculate the absorption length  $L_{\text{star}}$  in air of the star-producing radiation from the relative

TABLE I. Effect of scanning rate on accuracy.

Scanning hours	Objective	No. of 5 prong stars
5	$10\times$	33
7	$10\times$	42
9	$10\times$	46
24	$44\times$	51

\* Now at the University of Florida, Gainesville, Florida.

<sup>1</sup> Dilworth, Occhialini, and Payne, *Nature* **162**, 102 (1948).